

1 Supplementary table

Table S1: **Robustness of the theoretical predictions with respect to selection intensity**

Expansion with $N_{e,1}/N_{e,2} = 10$				Reduction with $N_{e,1}/N_{e,2} = 0.1$			
ρ	Theory	$\gamma_{min} = 250$ Mean (SE)	$\gamma_{min} = 20$ Mean (SE)	ρ	Theory	$\gamma_{min} = 250$ Mean (SE)	$\gamma_{min} = 20$ Mean (SE)
0.05	38.40	38.58 (0.34)	37.35 (0.33)	0.05	101.83	101.16 (0.66)	100.03 (0.65)
0.10	21.08	21.03 (0.19)	20.52 (0.19)	0.10	81.53	80.70 (0.50)	80.57 (0.49)
0.20	11.79	11.62 (0.10)	11.45 (0.10)	0.15	74.51	72.51 (0.45)	72.64 (0.46)
0.40	6.97	6.89 (0.06)	6.87 (0.06)	0.20	70.89	69.62 (0.43)	69.40 (0.43)
0.80	4.52	4.49 (0.04)	4.42 (0.04)	0.25	68.67	67.95 (0.42)	67.51 (0.42)

The models used in the simulations are the same as those described in Figures [S6](#) and [S7](#). In both cases, samples were taken from the population at time $t = 0.1$ after the change in population size, where t is expressed in units of $2N_{e,1}$ generations. We included neutral sites with different scaled recombination frequencies (ρ) with the selected site. The mean and standard error of the total branch length L for a sample of 20 alleles were estimated using 10,000 rounds of simulations.

2 Supplementary figures

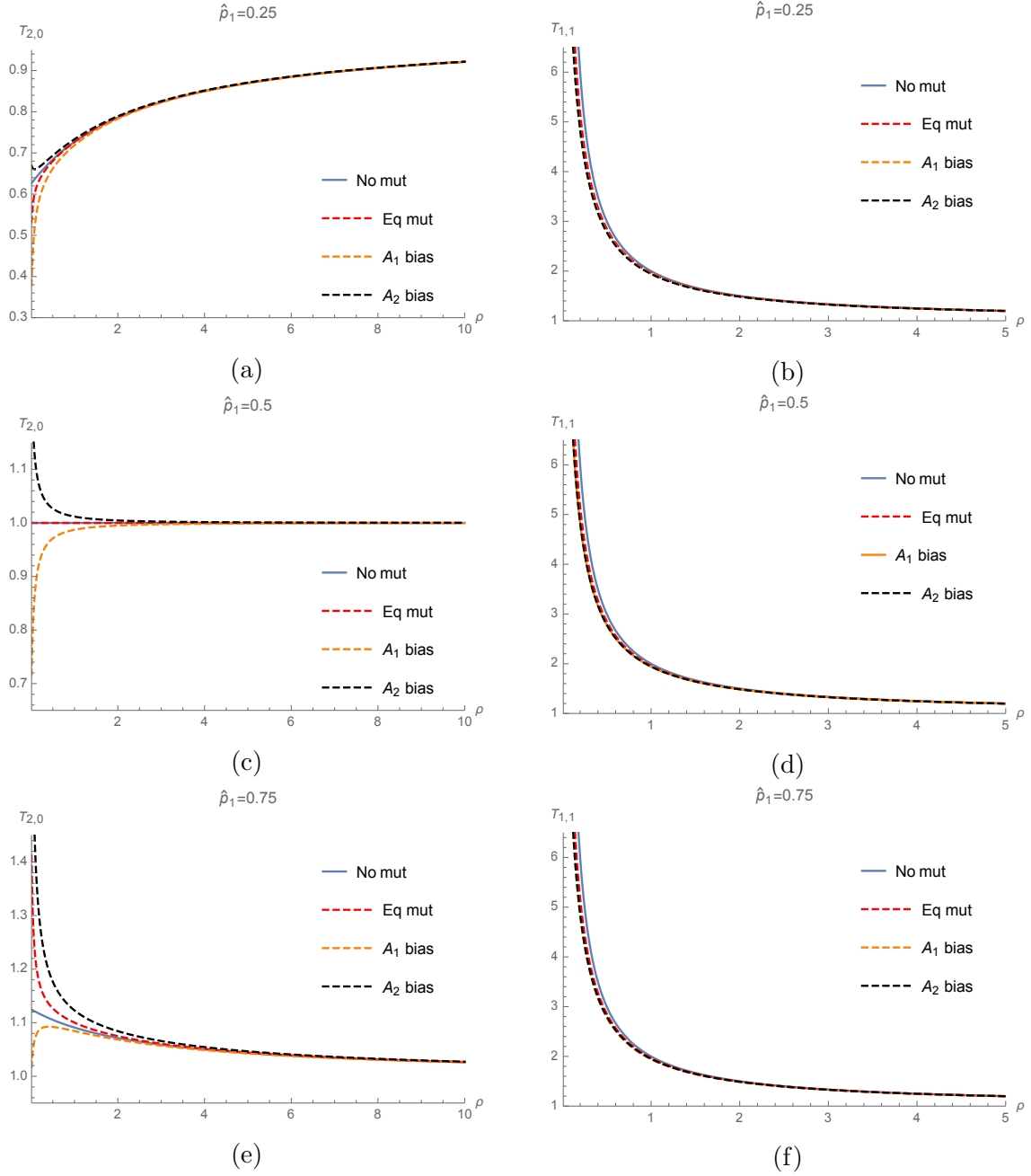
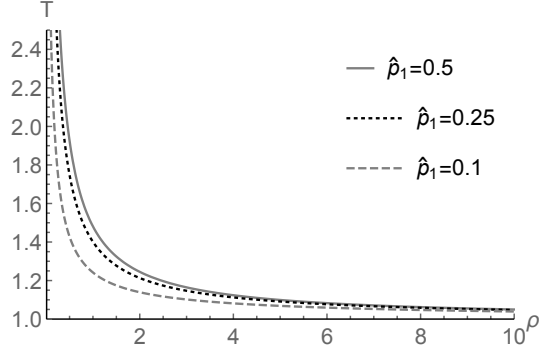
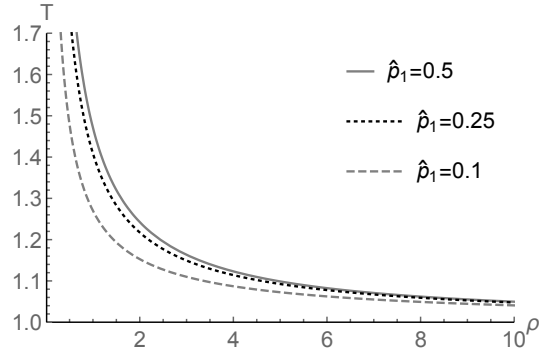


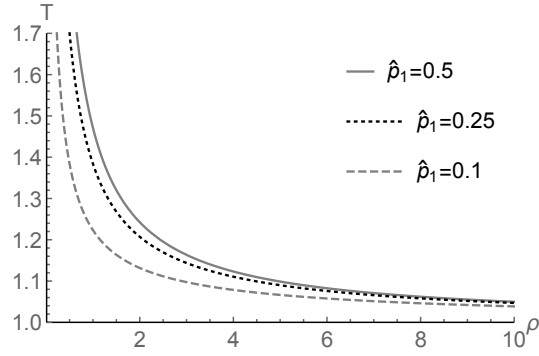
Figure S1: Expected coalescence time for a pair of alleles as a function of ρ . The selected alleles A_1 and A_2 are at equilibrium frequencies \hat{p}_1 and $1 - \hat{p}_1$. “No mut” means $\mu_{ij} = 0$ (i.e., (8)). “Eq mut” means $\mu_{ij} = 0.02$. “ A_1 bias” means $\mu_{12} = 0.01$ and $\mu_{21} = 0.05$. “ A_2 bias” means $\mu_{12} = 0.05$ and $\mu_{21} = 0.01$. The scales of the axes are different.



(a) Equal mutation rate



(b) A_1 bias



(c) A_2 bias

Figure S2: Expected coalescence time for a pair of alleles as a function of ρ . The selected alleles A_1 and A_2 are at equilibrium frequencies \hat{p}_1 and $1-\hat{p}_1$. “Equal mutation rate” means $\mu_{ij} = 0.02$. “ A_1 bias” means $\mu_{12} = 0.01$ and $\mu_{21} = 0.05$. “ A_2 bias” means $\mu_{12} = 0.05$ and $\mu_{21} = 0.01$.

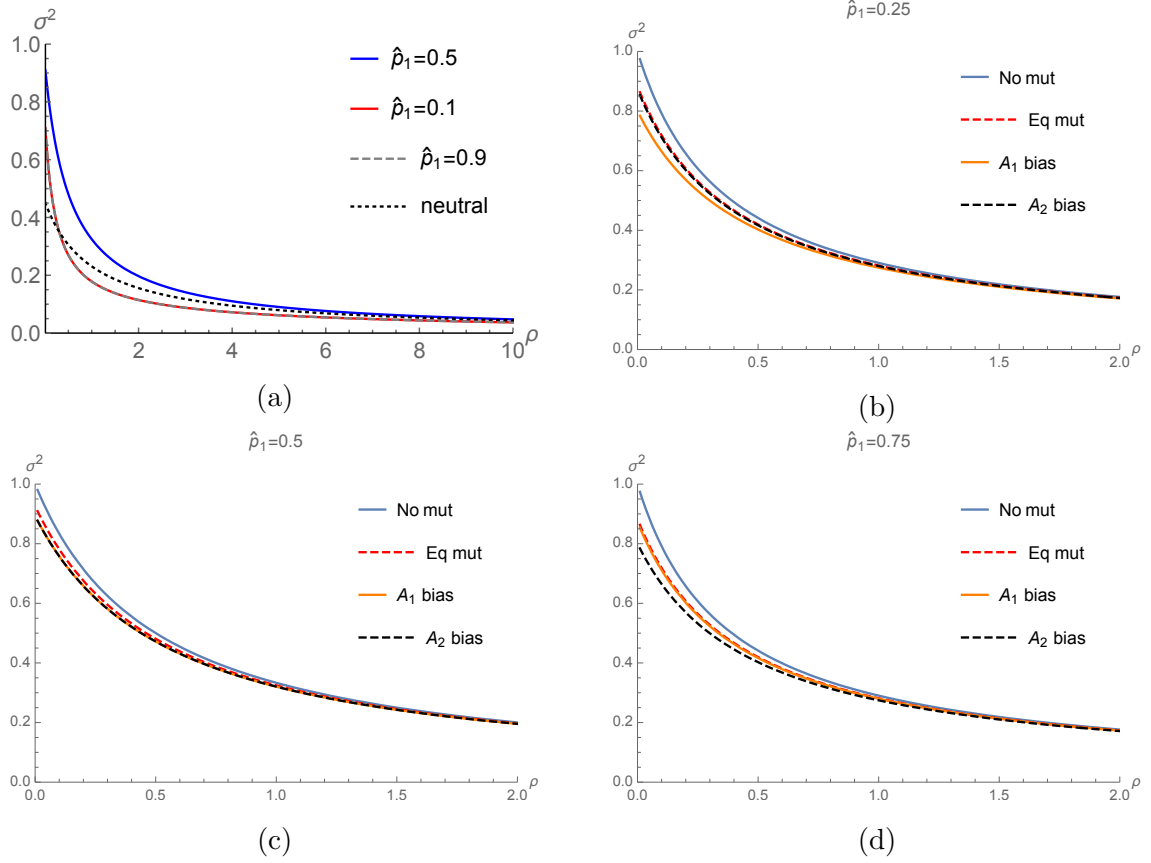


Figure S3: The level of LD between the selected and neutral loci as a function of ρ . In (a), the mutation rates between A_1 and A_2 are $\mu_{12} = \mu_{21} = 0.02$. In (b) - (d), for a given \hat{p}_1 , different mutation rates are considered. “No mut” means $\mu_{ij} = 0$. “Eq mut” means $\mu_{ij} = 0.02$. “ A_1 bias” means $\mu_{12} = 0.01$ and $\mu_{21} = 0.05$. “ A_2 bias” means $\mu_{12} = 0.05$ and $\mu_{21} = 0.01$.

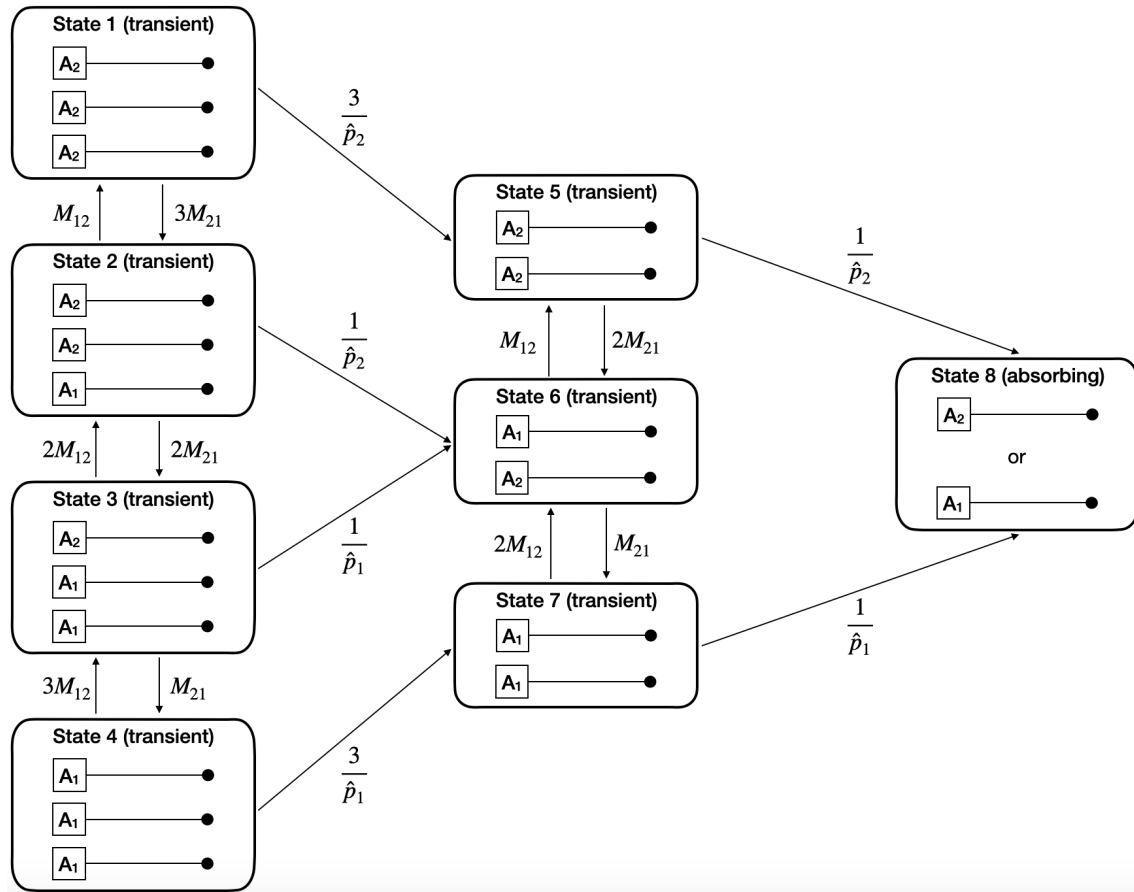


Figure S4: Transition rates between the states of the equilibrium balancing selection model for a sample of size three. Time is scaled in units of $2N_e$ generations. The neutral locus is represented by a black dot.

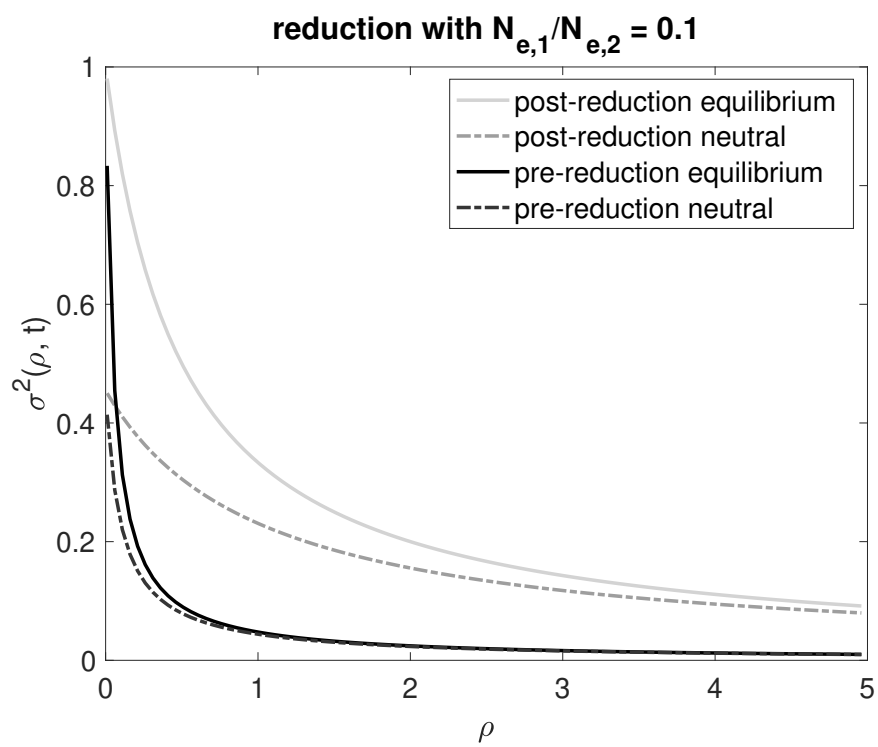


Figure S5: LD levels before and after population size reduction. The model is the same as that used in Figure 5d.

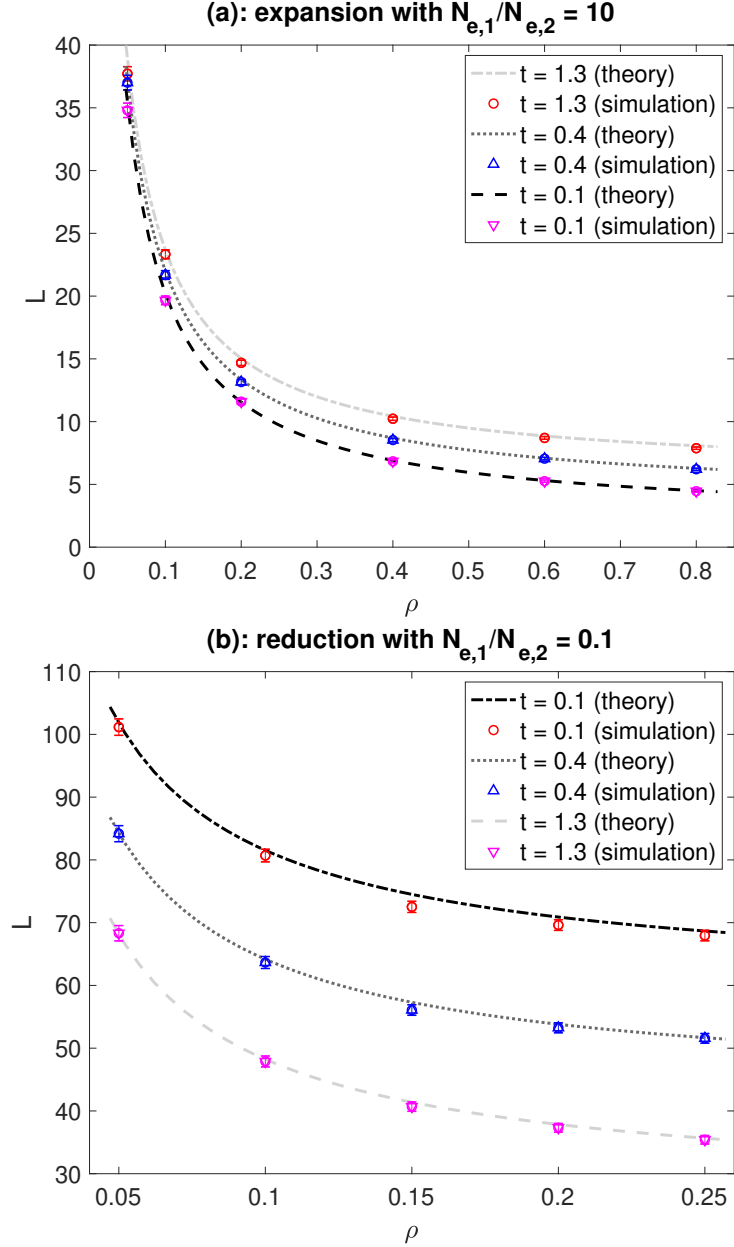


Figure S6: Expected total branch length L with demographic changes and strong balancing selection. We used the method described in the main text and Supplementary Text S.6 to carry out coalescent simulations with stochastic allele frequency trajectories, and compared the results to the theoretical predictions obtained under deterministic allele frequency trajectories. The population experienced a one-step change in population size at time t before the present. The population size in the present and ancestral epochs are $N_{e,1}$ and $N_{e,2}$, respectively. Time (t) and the recombination frequency (ρ) are expressed in units of $2N_{e,1}$ generations. For the expansion model in (a), $N_{e,1} = 20,000$ and $N_{e,2} = 2,000$. For the reduction model in (b), $N_{e,1} = 2,000$ and $N_{e,2} = 20,000$. These are the same as those considered in Figure 5. The fitnesses of A_1A_1 , A_1A_2 , and A_2A_2 are $w_{11} = 1 - s$, $w_{12} = 1$, and $w_{22} = 1 - s$, where $s = 0.0625$. We have $2 \min(N_{e,1}, N_{e,2})s = 250$, implying that selection is strong. The equilibrium frequencies of A_1 and A_2 are 0.5. The sample size is $n = 20$. The mutation rate from A_1 to A_2 is 6.25×10^{-8} per generation, and the rate in the opposite direction is the same. For each parameter combination, 10,000 simulation replicates were conducted to obtain an estimate of L . The whiskers show $L \pm 2 \times$ (standard error).

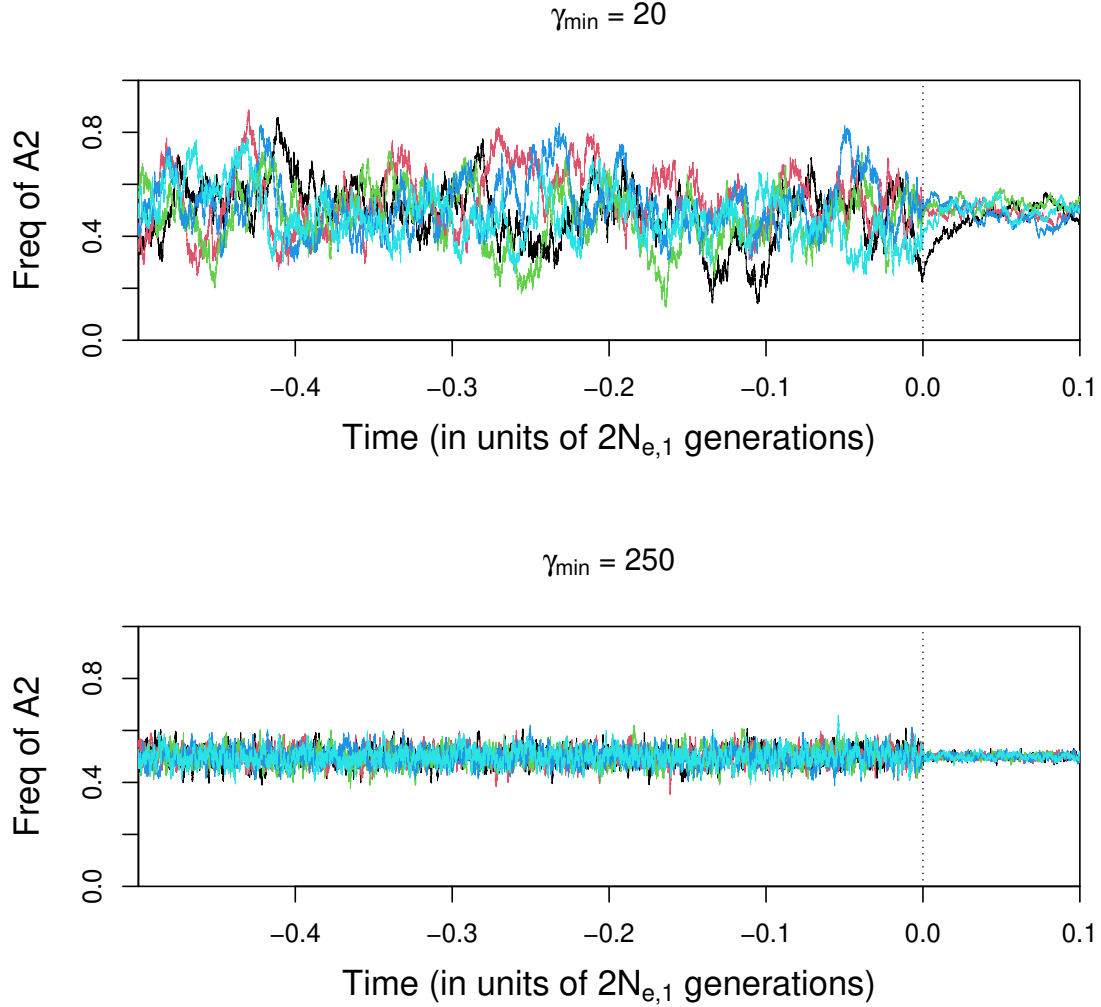


Figure S7: The effects of selection intensity on the extent of stochastic fluctuation in allele frequencies at the selected locus. We assumed the same population expansion model used in Figure S6, i.e., $N_{e,1} = 20,000$ (the current effective population size) and $N_{e,2} = 2,000$ (the effective population size in the ancestral epoch). The vertical dotted line indicates $t = 0$, which is when the population size increase takes place. The fitnesses of A_1A_1 , A_1A_2 , and A_2A_2 are $w_{11} = 1 - s$, $w_{12} = 1$, and $w_{22} = 1 - s$. Selection intensity is measured by $\gamma_{\min} = 2N_{e,\min}s$, where $N_{e,\min} = \min(N_{e,1}, N_{e,2})$. The mutation rate from A_1 to A_2 is 6.25×10^{-8} per generation, and the rate in the opposite direction is the same. For each parameter combination, allele frequency trajectories of A_2 were obtained using the forward simulation methods detailed in Supplementary Text S.6. In each plot, the trajectories from five simulations are included, and are shown in different colours.

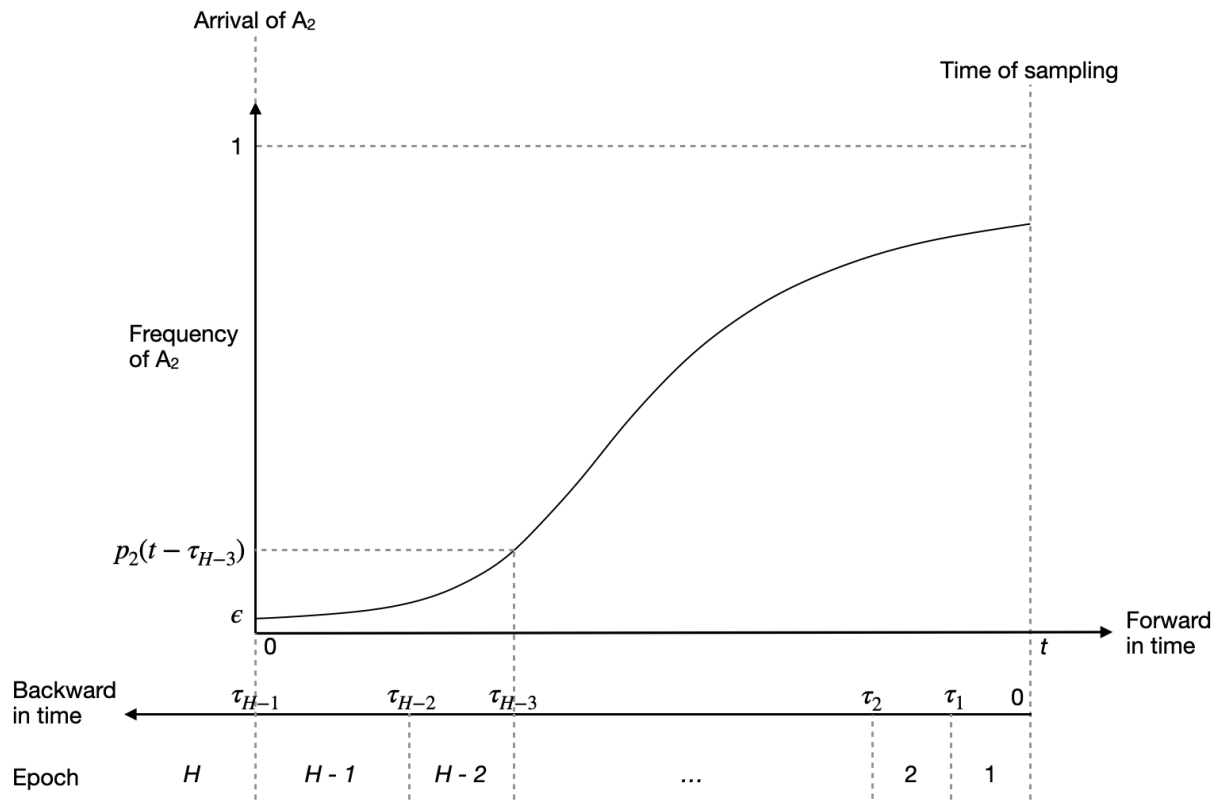
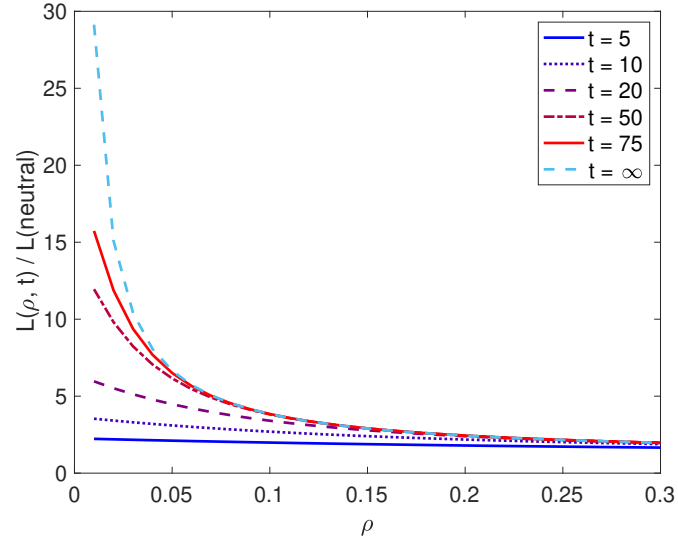
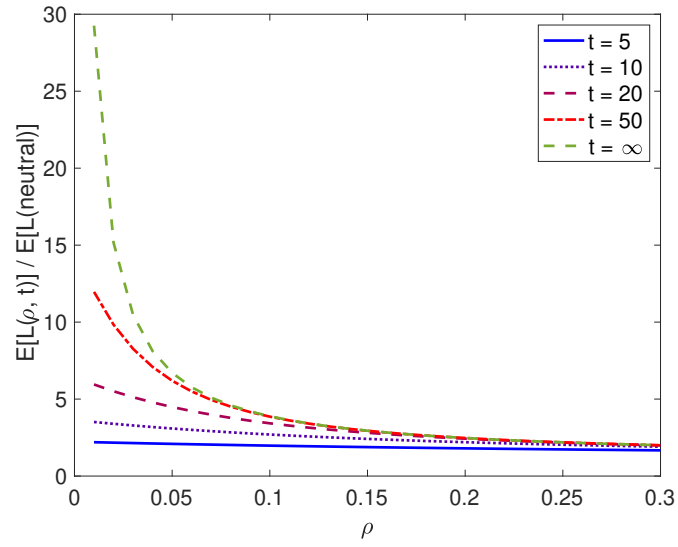


Figure S8: A diagram showing the discretisation scheme used to obtain the expected total branch length and the site frequency spectrum under the model of recent balanced polymorphism.



(a)



(b)

Figure S9: The approach to the equilibrium diversity level. The parameters are the same as those used in Figures 6 and 7. The sample size is 20. $\hat{p}_2 = 0.75$ in (a) and 0.5 in (b). Note that the curves are based on a model without reversible mutation between the two selected variants A_1 and A_2 . They overestimate the increase in diversity when ρ is very small.

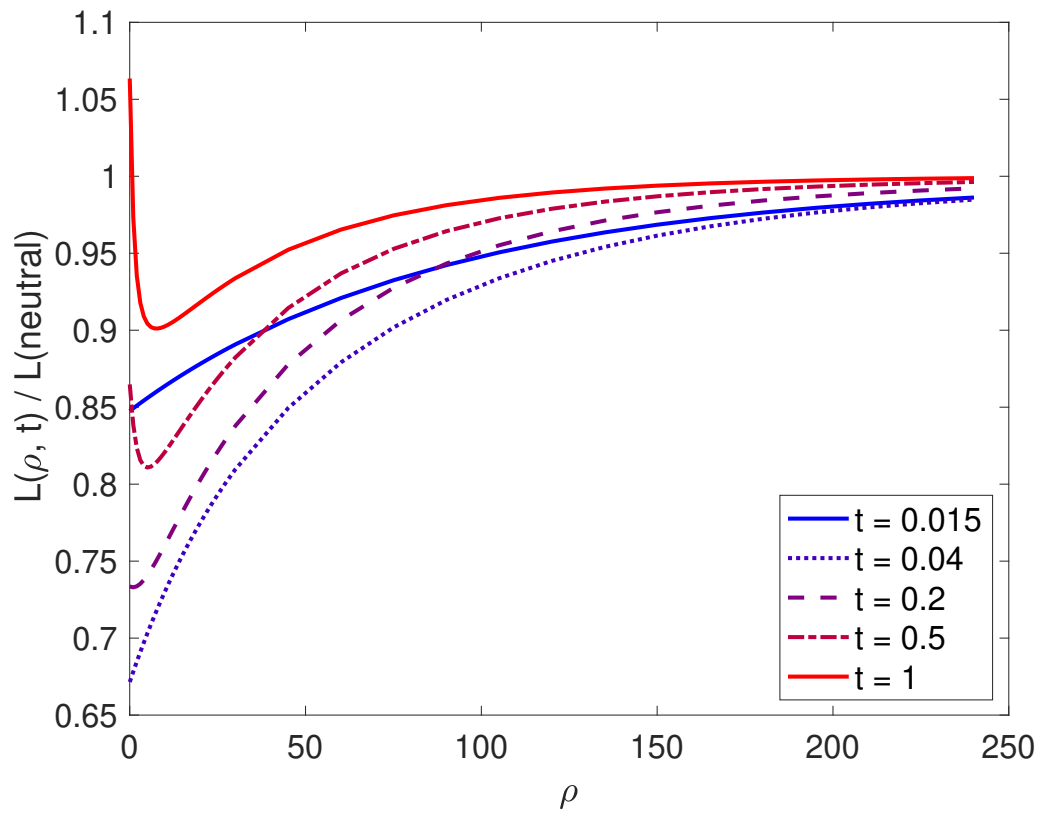


Figure S10: Neutral diversity in genomic regions surrounding a recently-emerged variant under balancing selection. The parameters are the same as in Figure 7 in the main text, except that the sample size is $n = 20$.

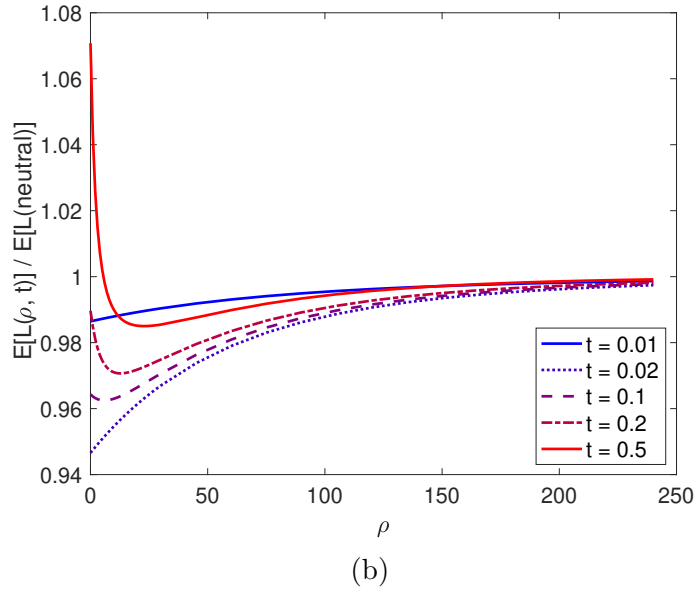
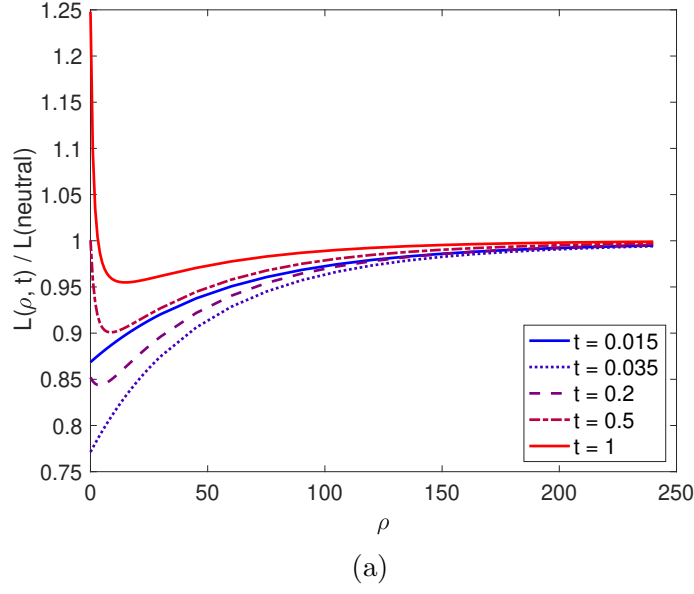


Figure S11: Neutral diversity level in genomic regions surrounding a recently-emerged balanced polymorphism. These figures are analogous to that in Figure 7, except that in (a) $\hat{p}_2 = 0.5$ and in (b) $\hat{p}_2 = 0.25$. The sample size is two.

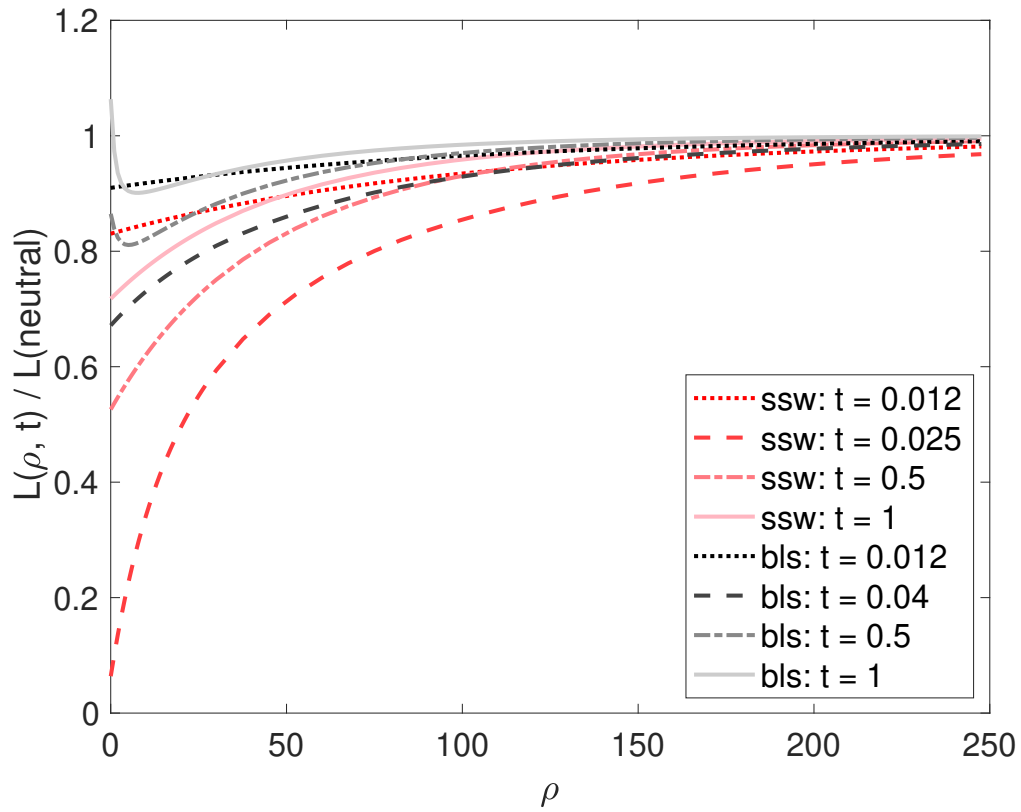
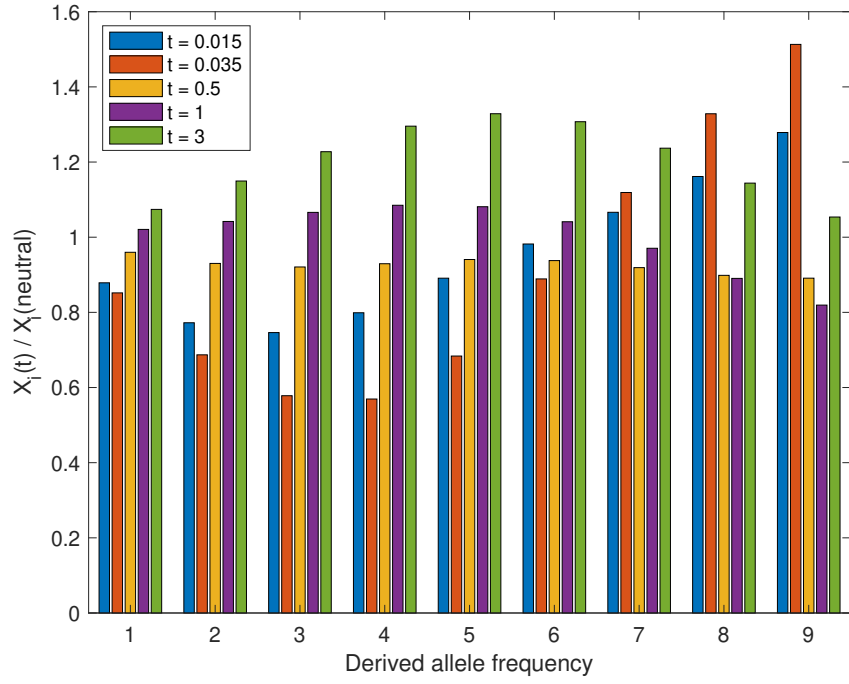
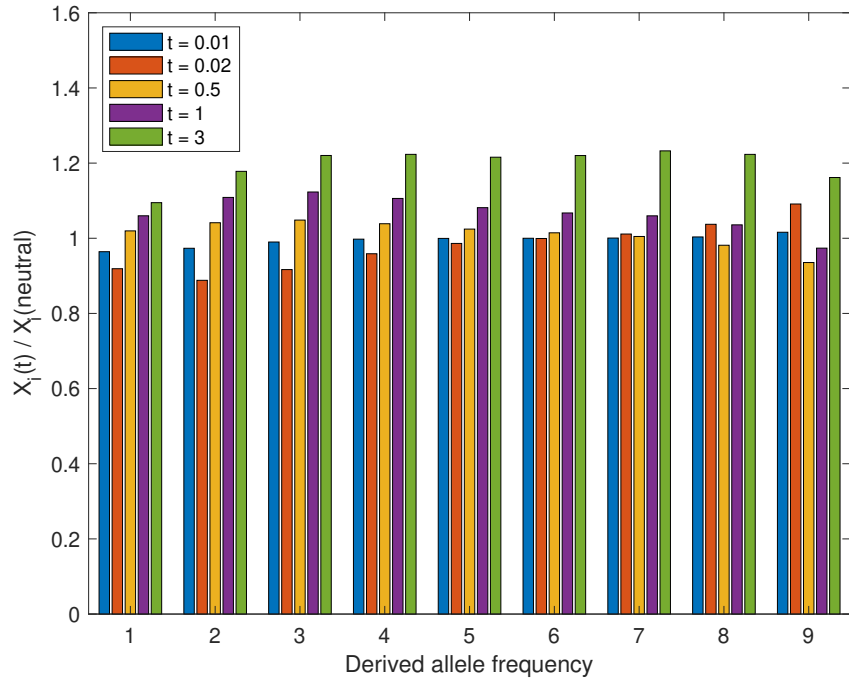


Figure S12: Comparing recent balancing selection with the corresponding sweep model with respect to their effects on diversity levels in surrounding genomic regions. The models and their parameters are the same as those in Figure 8, except that $n = 20$.



(a)



(b)

Figure S13: The SFS for the balancing selection models considered in Figure S11. In (a) $\hat{p}_2 = 0.5$ and in (b) $\hat{p}_2 = 0.25$.

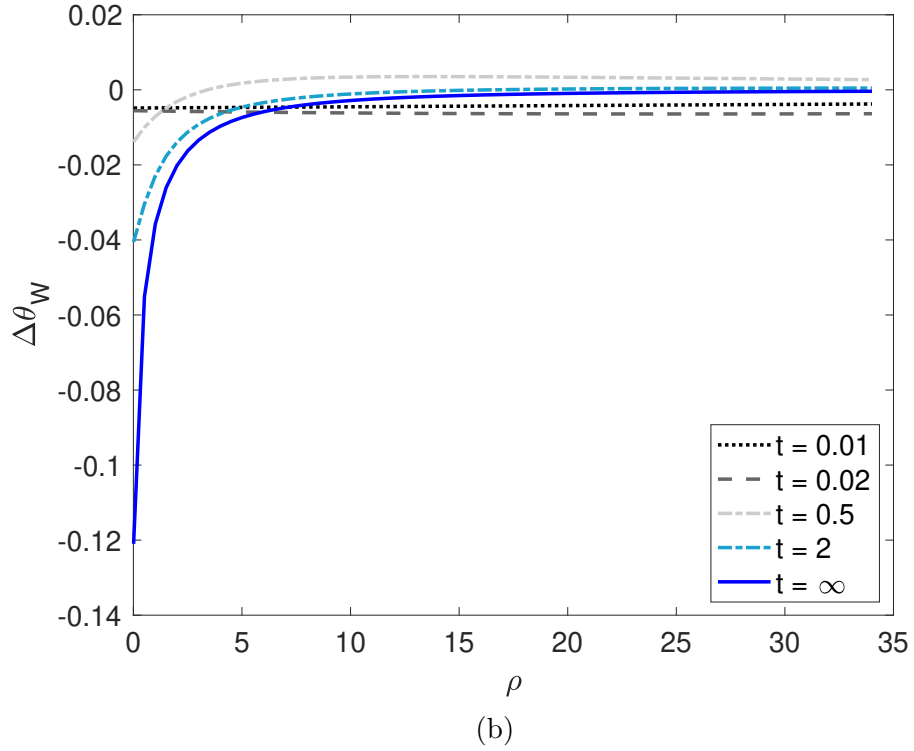
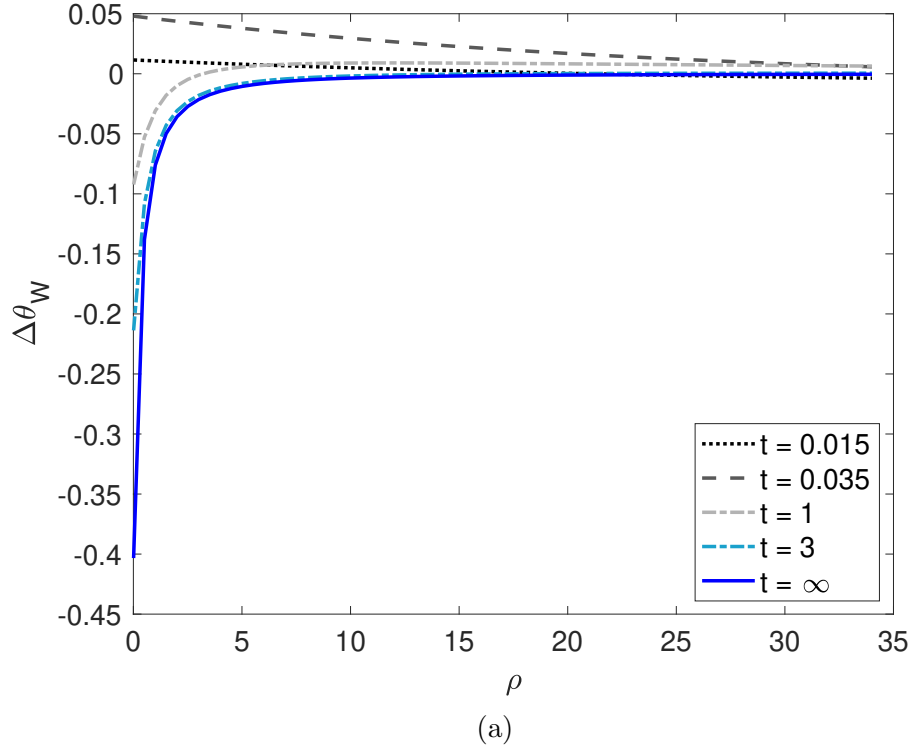


Figure S14: $\Delta\theta_W$ as a function of ρ and t for the balancing selection models considered in Figure S11. The sample size is 10. In (a) $\hat{p}_2 = 0.5$ and in (b) $\hat{p}_2 = 0.25$.

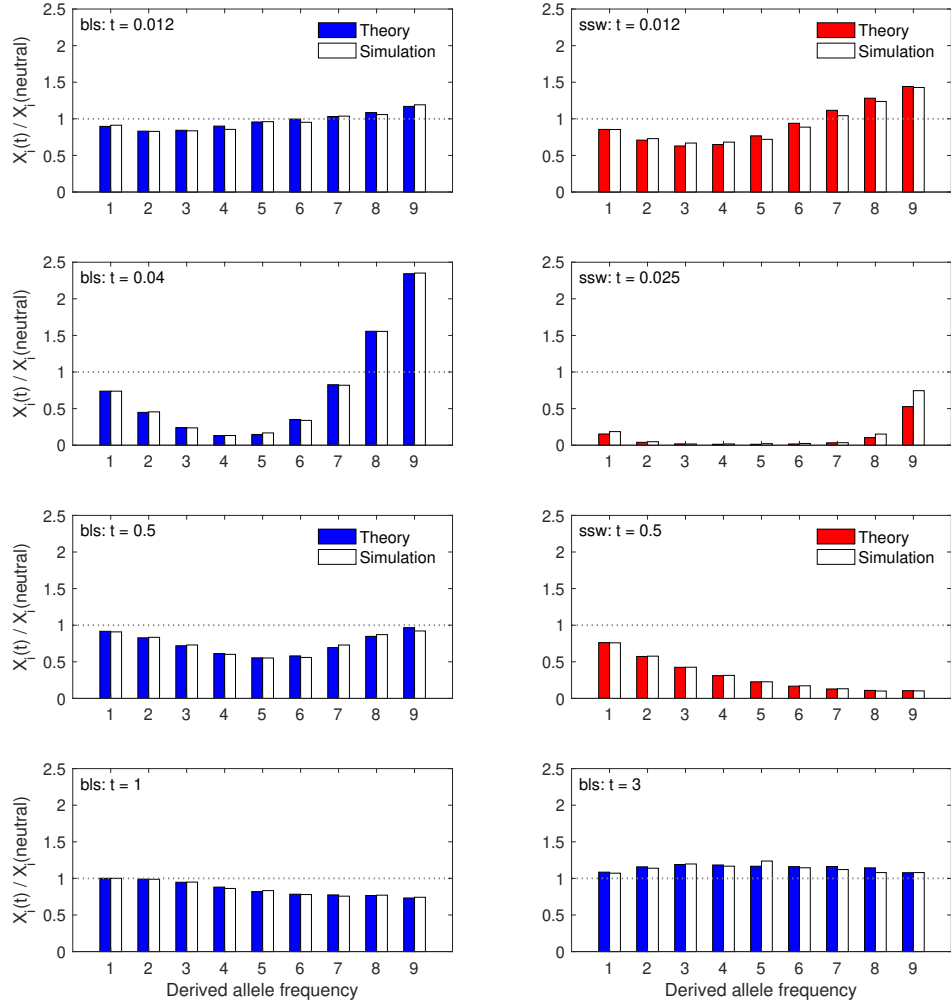


Figure S15: The SFS at various time points after the arrival of the selected variant for a sample of 10 alleles. The balancing selection (bls) and selective sweep (ssw) models are the same as those shown in Figure 9 in the main text (i.e., $\gamma_1 = 500$ and $\hat{p}_2 = 0.75$). The scaled recombination frequency between the focal neutral site and the selected site is $\rho = 2$.

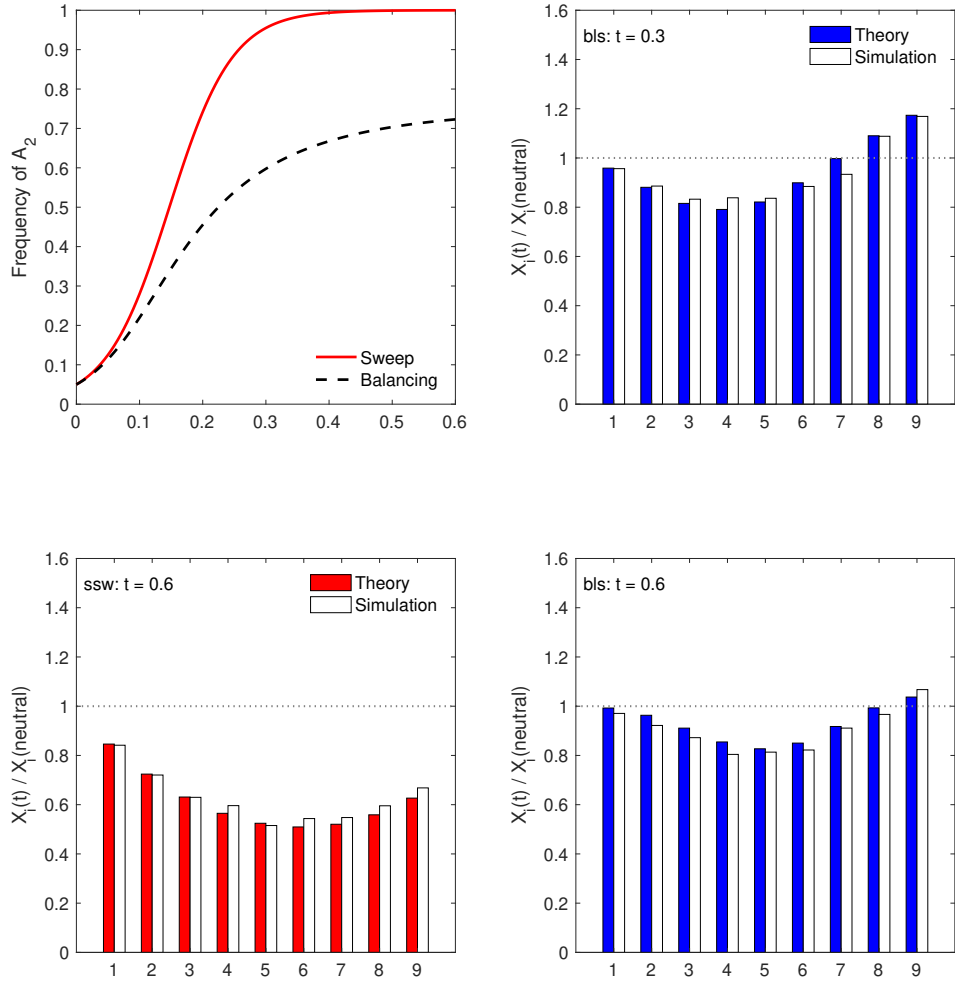


Figure S16: The SFS at various time points after the arrival of the selected variant for a sample of 10 alleles. The balancing selection (bls) model has $\gamma_1 = 20$ and $\hat{p}_2 = 0.75$, and the corresponding sweep (ssw) model was also simulated. The scaled recombination frequency between the focal neutral site and the selected site is $\rho = 2$.